Publ. Astron. Soc. Japan 24, 469-481 (1972)

Brightness Distribution of the Sun at 8.6 mm Wavelength

Kin-aki KAWABATA and Yoshiaki SOFUE

Department of Physics, Nagoya University, Nagoya

(Received 1972 May 1)

Abstract

The brightness distribution of the quiet sun at wavelength $\lambda=8.6$ mm is synthesized from off-meridian observations using a four element east-west interferometer with equal spacing of 273λ. The beam separation and the beam width of the interferometer are about 12.6 and 3 minutes of arc, respectively, at the meridian plane. The observed brightness distribution at 8.6 mm is essentially flat from the disk center to $0.95R_\odot$. In addition to the nearly uniform component over the optical disk there exists an excess component just outside the optical limb. The component outside the limb is in agreement with the coronal emissions at this wavelength. The physical condition of the spicules is discussed by comparing the present observational data with the plane-parallel models of the chromosphere by GINGERICH and DE JAGER (1968; BCA) and by VERNAZZA and NOYES (1972). The present data indicate that the electron temperature in the spicules is less than 6000 K, which agrees with HIRAYAMA's (1971) value, 6000-8000 K, but contradicts the value of 16000 K derived by BECKERS (1968) from optical observations.

Key words: Brightness distribution of the Sun; Interferometer; Model chromospheres; Spicules.

1. *Introduction*

The quiet-sun radiations at millimetric wavelengths provide information on thermal properties in the solar chromosphere. The dependence of the brightness temperature at the disk center on wavelengths has been widely used to place restrictions on models of the chromosphere. Center-to-limb variations of the millimetric radiation also give important clues to the physical condition of the chromosphere.

HAGEN (1951) has calculated the distribution of the brightness temperature at these wavelengths, predicting a limb brightening. A considerable number of observations of brightness distributions at millimetric and short centimetric wavelengths have been made. Table 1 summarizes observations at millimetric and short centimetric wavelengths. At the millimetric wavelengths, no systematic secant-like limb brightening has been obtained but most of the available observational data suggest that the brightness distribution is flat up to $0.9R_\odot$ from the disk center. In addition, COATES, GIBSON, and HAGEN (1958) have reported a darkening at 0.6 to $0.9R_\odot$. Some observations have indicated the existence of a little spiky brightening at the limb.

COATES (1958b) has pointed out that plane-parallel models of the chromosphere are insufficient to interpret the observed radio brightness distributions and inhomogeneous structures such as spicules must be taken into account. Recently, SIMON and ZIRIN (1969) have argued that model chromospheres such as GINGERICH and DE

TABLE 1. Summary of Observations of the Center-to-Limb Brightness Distributions at Millimetric and Short Centimetric Wavelengths.

Wavelength	Reference	Results	Method
1.2 mm.....	NOYES, BECKERS, and LOW (1968)	Evidence of limb brightening	
1.2 mm.....	NEWSTEAD (1969)	High limb brightening	Eclipse, 1966; 1.6 mϕ dish
1.2 mm.....	KUNDU (1971)	Limb darkening	Scanning with 36 ft ϕ dish
1.4 mm.....	SHIMABUKURO (1971)	Little or no limb brightening	Scanning with 15 ft ϕ dish
3.2 mm.....	TOLBERT, KRAUSE, and STRACHAN (1964)	No systematic limb brightening	Eclipse; 60 inch search-light antenna
3.2 mm.....	SIMON (1965)	Limb brightening$\lesssim$ 1 % of disk center	Scanning with 15 ft ϕ dish
3.2 mm.....	TAKAHASHI (1967)	$R_{3.2\mathrm{mm}}=1.155\,R_\odot$	Scanning with 15 ft ϕ dish
3.3 mm.....	SHIMABUKURO (1970)	$R_{3.3\mathrm{mm}}=R_\odot+7000$ km for E-W; $R_{3.3\mathrm{mm}}$ is slightly greater than $R_\odot$ for N-S	Scanning with a pencil beam of 2′.8
3.4 mm.....	SIMON, BUHL, COGDELL, SHIMABUKURO, and ZAPATA (1970)	Limb brightening$\leq$ 1% of disk center	Eclipse, 1969; 15 ft ϕ dish
3.5 mm.....	TLAMICHA (1969)	No direct evidence of limb brightening	Scanning with 36 ft ϕ dish
4.3 mm.....	COATES (1958a)	Uniform disk with $R_{4.3\mathrm{mm}}=(1.01\pm0.005)\,R_\odot$	Scanning with 10 ft ϕ dish
4.3 mm.....	TAKAHASHI (1967)	$R_{4.3\mathrm{mm}}=1.021R_\odot$	Scanning with 15 ft ϕ dish
4.3 mm.....	TLAMICHA (1969)	No direct evidence of limb brightening	E-W and N-S scannings with 36 ft ϕ dish
8.6 mm.....	COATES, GIBSON, and HAGEN (1958)	Limb spike of 10% of disk center at $R=1.007\,R_\odot$; Darkening at 0.6-0.9 $R_\odot$	Eclipse, 1954; With a fan beam
8.6 mm.....	SALOMONOVICH, PARIISKY, and KHANGIL'DIN (1958)	$R_{8.6\mathrm{mm}}=R_\odot+6000$ km: Slight limb spike: Darkening at $\sim0.8\,R_\odot$	Eclipse, 1954
8.6 mm.....	TAKAHASHI (1967)	$R_{8.6\mathrm{mm}}=1.04\,R_\odot$	Scanning with 15 ft ϕ dish
8.6 mm.....	Present work	Uniform disk and Coronal component	E-W grating interferometer with fan beam 3′
9 mm.....	FLETT, FOSTER STRACHAN, and THORNTON (1971)	Total limb brightening flux $\leq$5% of total disk flux	Eclipse, 1971; 4.5 mϕ dish
1.18 cm	EL-RAEY (1971)	No limb brightening: High coronal contribution	Eclipse, 1971; 20 ft ϕ dish

TABLE 1. (Continued)

Wavelength	Reference	Results	Method
1.35 cm.....	SIMON, BUHL, COGDELL, SHIMABUKURO, and ZAPATA (1970)	Clear evidence of limb brightening	Eclipse, 1969; 120 ft ϕ dish
2.0 cm.....	TLAMICHA (1969)	No direct evidence of limb brightening	Scanning with 140 ft ϕ and 120 ft ϕ dishes

JAGER (1968) or the ALLEN (1963) model are insufficient to interpret the observed brightness distributions in the wide range of spectra from the millimetric to the ultraviolet region. They have emphasized the importance of inhomogeneous structures for the interpretation of the brightness distributions.

The purpose of the present paper is to report an observation of the brightness distribution of the quiet sun using the east-west interferometer at the wavelength 8.6 mm with a resolution of 3 minutes of arc. In conformity with the present observational data, physical conditions in spicules are discussed.

2. *Instrument and Observations*

The instrument is an east-west grating interferometer and consists of four fixed 40 cm diameter paraboloidal mirrors with Cassegrain feed systems and four plane mirrors of equatorial mountings (Figure 1). Each paraboloidal mirror is fixed pointing downwards along a polar axis of the respective plane mirror which is placed in front of each paraboloidal mirror. This particular system of antennas eliminates the need for waveguide rotary joints while still allowing the antennas to point towards the sun at all the times.

The four antennas are placed along an east-west line with an equal spacing of D=234 cm (273λ) between each other. After signals from a pair of two adjacent antennas are added by connecting these antennas with a rectangular waveguide of standard size, they are transmitted to a common receiver through rectangular waveguides twice as large as the standard size in order to reduce transmission loss. The receiving system is a ferrite-modulated Dicke radiometer and a balanced mixer with a 130 MHz IF amplifier (10 MHz band width) is used.

The antenna spacing of 273λ for the four-element grating interferometer corresponds to a beam separation of about 12.6 minutes of arc and a half beam width of about 3.1 minutes of arc at the meridian plane. Time intervals of observations due to a drift scanning are about 50 seconds at the meridian transit. The selection of the large spacing of the interferometer is made in order to get short time intervals of the drift scanning and a long observing time. In order to get a long observing time, we have to note that obscuration of each antenna by an adjacent one prohibits observations at large angles from the meridian plane. The antenna spacing of 273λ is selected to get a large amplitude of the interference pattern of the quiet sun at the meridian transit, which make it easy to measure phase errors of our instrument.

The instrument has been constructed primarily for studying 8.6 mm bursts, but it provides also useful information on the quiet sun. Our instrument gives only

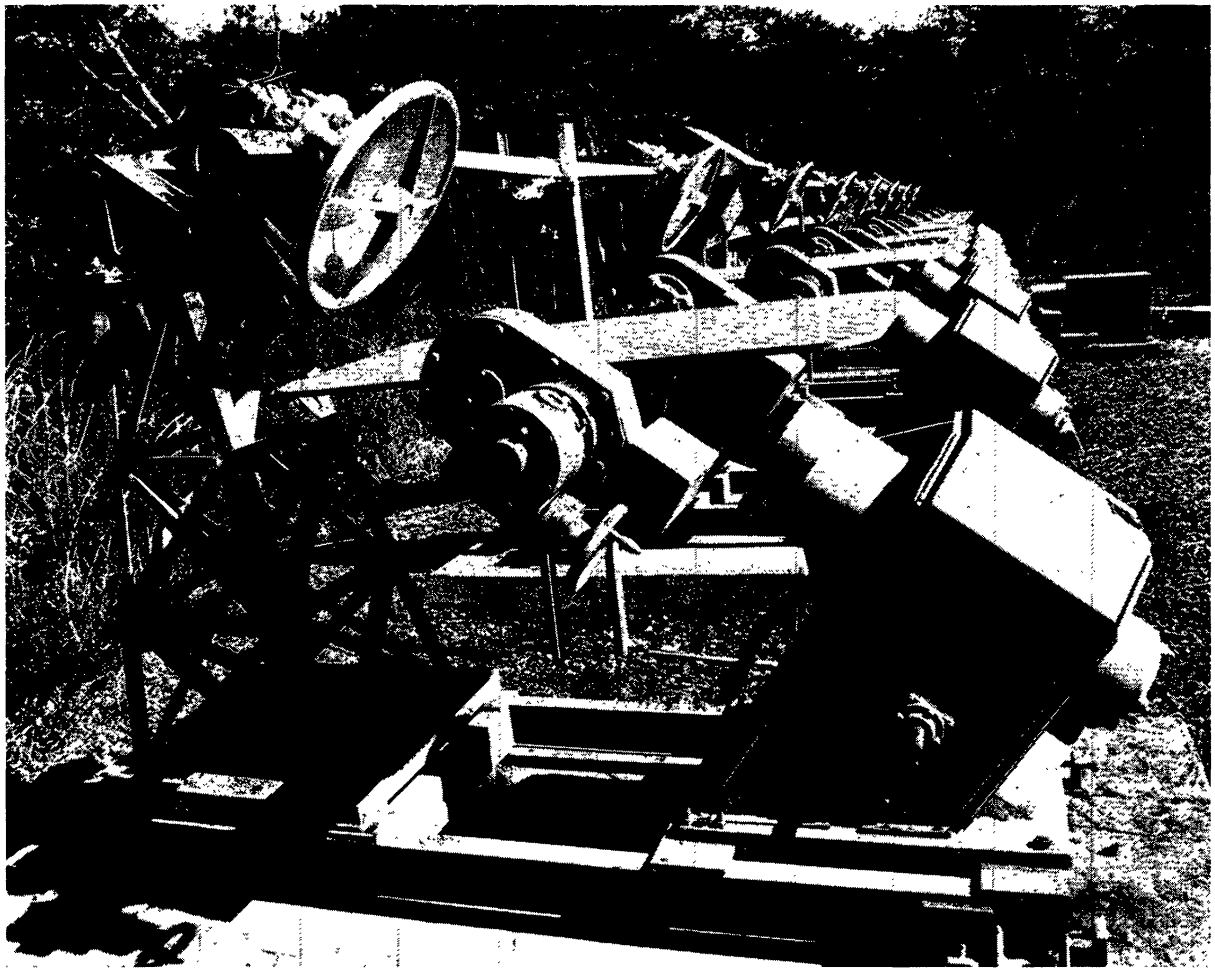

FIG. 1. 35 GHz interferometer at the Department of Physics, Nagoya University. The instrument has been extended to an eight-element interferometer.

higher Fourier components of the brightness distribution at the meridian plane, but the decrease of the effective spacing between antennas at large angles from the meridian plane enables us to measure low Fourier components. Thus we can synthesize the brightness distribution of the quiet sun by utilizing observations throughout a day. All the required Fourier components can be observed only around the equinox by our instrument, and then we select the data on April 7, 1971 to synthesize the brightness distribution of the quiet sun. This day was one of the most quiet days of the sun (see, e.g. Aeronomy and Space Data Center 1971) and, also, we had the best weather condition of this particular period.

3. *Synthesis of the Brightness Distribution of the Quiet Sun*

Since our observation of the sun has been made by east-west fan-beam interferometer, we synthesize the brightness distribution of the quiet sun assuming circular symmetry of the distribution. Let $B(r)$ be the brightness of the sun at an angular distance, r, from the disk center. The brightness of the sun should decrease rapidly outside the optical limb at 8.6 mm. Then it is permissible to assume

$B(r)$ vanishes at a periphery, $r=R$, which is located sufficiently far from the solar disk.

Then the brightness distribution, $B(r)$, can be expanded by using the zero-order Bessel functions as

$$B(r)=\sum_{i=1}^{\infty} B_i J_0(\mu_i r/R) \quad \text{for} \quad r\leq R\ , \tag{1}$$

where μ_i represents i-th zero of the zero-order Bessel function, i.e.,

$$J_0(\mu_i)=0\ . \tag{2}$$

As is well known, the coefficients, B_i, in this series expansion are given by

$$B_i=\frac{1}{R^2 J_1^2(\mu_i)}\int_0^R rB(r)J_0(\mu_i r/R)dr\ . \tag{3}$$

It can be easily shown that the coefficients, B_i, in equation (1) relate to the visibility function, $a(\kappa)$, as

$$\frac{B_i}{B_0}=\frac{1}{R^2 J_1^2(\mu_i)}a(\mu_i/R)\ , \tag{4}$$

where $\kappa=nDR_\odot\cos\Theta/\lambda(n=1,\ 2,$ and 3 for our instrument). Here D, $R_\odot$, λ, and Θ represent the spacing between antennas, the angular diameter of the optical sun, the wavelength, and the angle from the meridian plane to the sun, respectively, and

$$B_0=2\int_0^R rB(r)dr \tag{5}$$

represents the mean brightness of the sun.

Therefore B_i/B_0 can be obtained from the visibility function, if we choose the angle from the meridian plane to the sun properly for respective values of i. In the present paper, R is taken as 1.2 times the solar radii. Using this selection of R, our instrument gives B_i/B_0 up to $i=9$. The B_i/B_0 for $2\leq i\leq 9$ are evaluated by this procedure, and B_1/B_0 is determined so as to satisfy the equation

$$2\int_0^R r\sum_{i=1}^{9}\frac{B_i}{B_0}J_0(\mu_i r/R)dr=1\ . \tag{6}$$

The values of B_2/B_0 and B_3/B_0 can be determined from both the fundamental and the second harmonics of the interference patterns of the sun by our instrument. Similarly, B_4/B_0, B_5/B_0, and B_6/B_0 can be determined from both the second and the third harmonics of the observed patterns. By comparing these values of B_i/B_0 determined from each the harmonic of the observed patterns, we can check the phase and amplitude errors of our instrument.

Then the brightness distribution of the sun can be obtained by taking a partial sum of equation (1) up to $i=9$. The calculation of the brightness is made at $r=r_j$, where r_j satisfies

$$J_0(\mu_{10}r_j/R)=0\ , \tag{7}$$

because the calculated brightness at these points is correct up to the 10-th order term. Using the calculation of the partial sum, we can take the Cesàro sum in

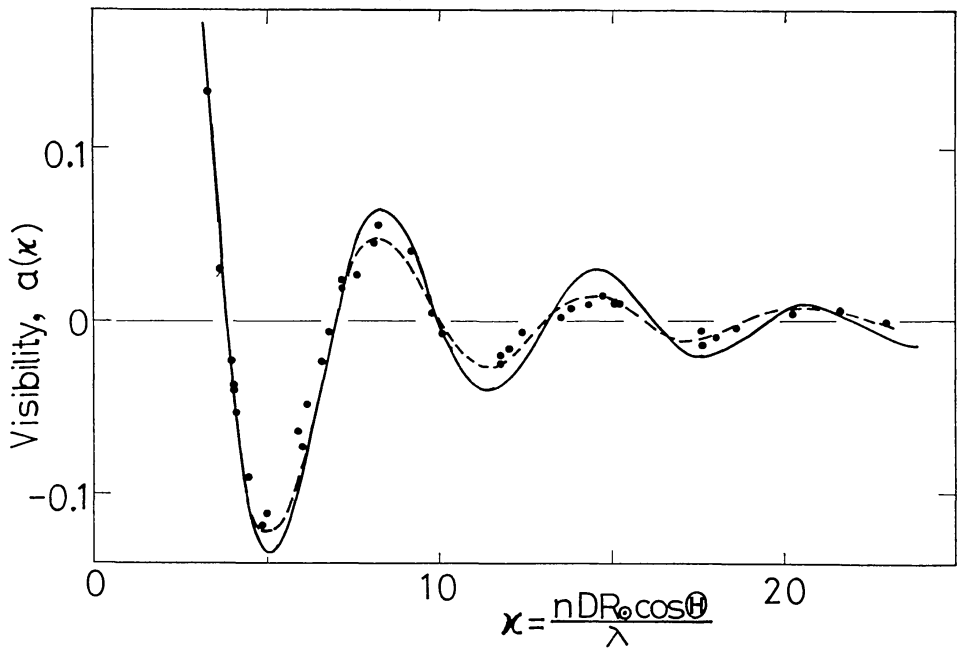

FIG. 2. The dependence of visibility on the effective antenna spacings. Dots: Observed values. Solid line: Calculated values for the uniform brightness distribution over the circular disk with a radius of $1.015\,R_\odot$. Dashed line: Calculated values by equation (1) using observed values of B_i/B_0.

order to improve the oscillation close to the limb due to the Gibbs phenomena.

The dependence of the visibility function, $a(\kappa)$, on κ is illustrated in Figure 2. Dots in the figure indicate observed values of the visibility and the dotted line represents a calculated one by using B_i/B_0 determined by the procedure described above.

If we assume the brightness distribution at 8.6 mm is uniform over a circular disk with a radius $R_{8.6\text{mm}}$, then the best fit with observations is achieved for $R_{8.6\text{mm}}=1.015R_\odot$, which corresponds to a height of 10500 km above the optical limb. The present value of the effective radio size of the sun is small compared with that of $1.04R_\odot$ observed by TAKAHASHI (1967) at 8.6 mm using a 15 ft paraboloidal antenna. The same fitting with observations is achieved as well, if there exists a limb spike with a flux of 3 percent of the total flux in addition to the uniform component over the optical sun. This value of the flux of a limb spike is in agreement with an upper limit of 5 percent obtained from an eclipse observation at 9 mm by FLETT, FOSTER, STRACHAN, and THORNTON (1971).

The solid line in Figure 2 is the theoretical curve of the visibility function for a uniform distribution over the circular disk of radius $1.015R_\odot$, as well as for a composite of uniform distributions over the optical sun and a limb spike with a flux of 3 percent of the total flux. As is seen in the figure, these distributions do not sufficiently reproduce the observed values of the visibility function. Then such simple distributions will be unrealistic.

Figure 3 demonstrates the difference, $\Delta B(r)/B_0$, between the observed brightness and the same partial sum of equation (1) for a uniform distribution of brightness over the optical sun. It is seen in the figure that the observed brightness is essentially flat from the disk center to $0.95R_\odot$. In addition to the nearly uniform

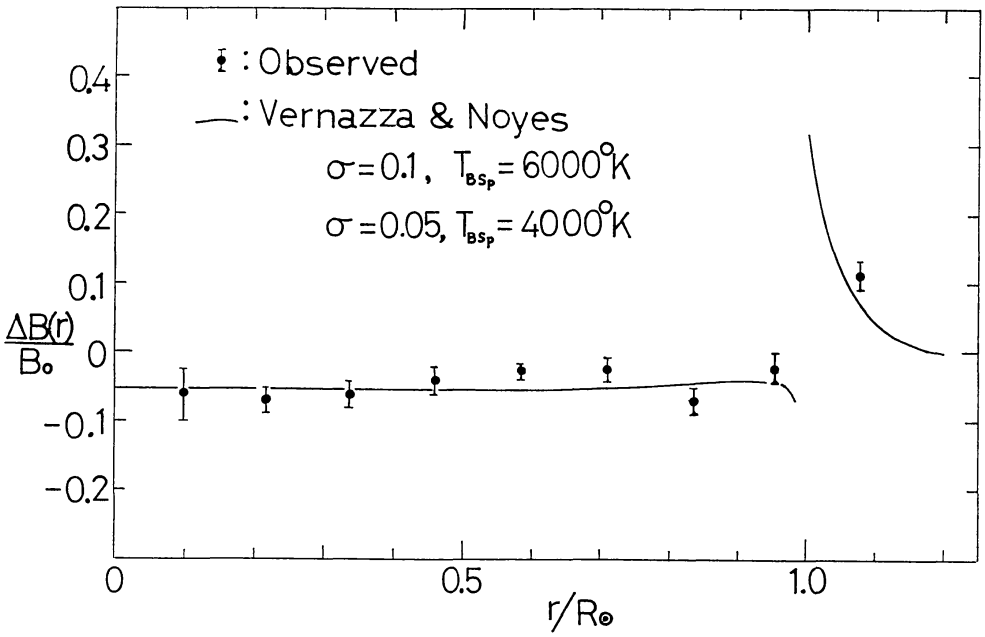

FIG. 3. The excess of brightness from a uniform distribution over the optical disk. Dots: The difference, $\Delta B(r)/B_0$, between the observed brightness distribution and the same partial sum of equation (1) for a uniform distribution of brightness over the optical disk. Lengths of bars indicate probable errors. Solid line: Calculated from a model described in Section 4.

component over the optical disk, an excess component just outside the limb is evident.

The solid line in Figure 3 represents a theoretical brightness in excess of the uniform distribution over the optical disk. The calculation of the theoretical brightness is described in Section 4. By comparing observations with the calculation, the component outside the limb is in agreement with the coronal emissions.

COATES, GIBSON, and HAGEN (1958) and SALOMONOVICH, PARIISKY, and KHANGIL'DIN (1958) have reported a darkening at 0.6–0.9$R_\odot$ from the disk center. The present observation also indicates a slight depression of brightness at 0.8$R_\odot$. It is, however, still open to question whether the depression really exists or not because of a lack of accuracy.

4. *Comparison with Models of the Solar Chromosphere*

It has been demonstrated by COATES (1958b) that a plane-parallel atmosphere fails to interpret either the radio spectrum or the center-to-limb variation at millimetric wavelengths, and that a cold inhomogeneous component must be taken into account. He has attributed the cold component to spicules and has concluded that the temperature in spicules is about 6400 K.

Recently, SIMON and ZIRIN (1969) have emphasized the importance of the inhomogeneous structure for the interpretation of the brightness distributions in the wide range of spectra from tne millimetric to the ultraviolet region. WITHBROE (1970) has argued for spicular absorption by using the center-to-limb variation data on the XUV lines of the ions C III, N III, N IV, O III, O IV, O V, and Si IV, and

VERNAZZA and NOYES (1972) have performed a similar analysis using the center-to-limb variation data of the Lyman continuum radiations. VERNAZZA and NOYES (1972) have suggested, furthermore, that the electron temperatue in spicules will be below 5200 K in accordance with the limb darkening at 1.2 mm observed by KUNDU (1971).

The emitting region of millimetric radiations in the solar chromosphere is a thin layer having a thickness as thin as a few hundred km at a height of about 2000 km or less. The height of an emitting layer of millimetric radiations is well below the average height of spicules, 4000 km. If spicules are opaque to the radiations under consideration, the absorption modifies the brightness distributions of the chromospheric component of these radiations. For the coronal component of millimetric radiations, the effect of absorption by spicules can be ignored, because the scale height of the solar corona is much larger than the average height of the spicules.

If spicules are opaque to radiations, the observed brightness temperature can be approximated by

$$T_B = PT_{\mathrm{Ch}} + (1-P)T_{\mathrm{Sp}} + T_{\mathrm{Cor}} , \tag{8}$$

by taking into account the effect of obscuration of the plane-parallel chromosphere due to spicules and emissions from spicules. Here T_{Ch}, T_{S}, and T_{Cor} represent the brightness temperature of the plane-parallel chromosphere, of the spicules, and of the corona, respectively, and P denotes the fraction of the area at an angle θ not obscured by spicules in the line of sight to the earth.

Now we suppose that spicules have a cylindrical structure of diameter, d, and height, h, and they are distributed randomly over the solar surface with a mean surface density, N_s. Furthermore, we assume that the number of spicules with height, h, is proportional to $\exp(-h/H)$, where H denotes the average height of the spicules. We ignore the correction for the curvature of the solar surface. Then we obtain

$$P = \exp\left(-\sigma \tan\theta - \frac{N_s d^2}{4}\right) , \tag{9}$$

where $\sigma = N_s d \exp(-H_{\mathrm{Ch}}/H) H$

$$\approx N_s d(H - H_{\mathrm{Ch}}) \quad \text{for} \quad H_{\mathrm{Ch}} \ll H . \tag{10}$$

Here H_{Ch} represents the height of the radio emitting layer in the plane-parallel chromosphere.

DUNN (1960) has obtained the width of the spicules to be 1.2 seconds of arc, which corresponds to 815 km, from his observations at Sacramento Peak Observatory. Since the cross section of a spicule is very small, the second term in the exponent of equation (9) can be ignored. Thus the fraction of the area P is a function of the parameter $\sigma = N_s d(H - H_{\mathrm{Ch}})$ alone. WHITHBROE (1970) has found $\sigma = 0.05$ for spicules and $\sigma = 0.10$ for dark mottles, using $N_s = 3.3 \times 10^{-8}\,\mathrm{km}^{-2}$, $H = 4000$ km, and $d = 825$ km for spicules and $N_s = 4.9 \times 10^{-8}\,\mathrm{km}^{-2}$, $H = 5000$ km, and $d = 700$ km for the dark mottles.

The brightness temperature of the plane-parallel chromosphere is given by

$$T_{\mathrm{Ch}} = \int_0^\infty T \exp(-\tau \sec\theta) d\tau \sec\theta , \tag{11}$$

where

$$\tau = \frac{\xi}{\nu^2} \int_z^\infty \frac{N_e^2}{T^{3/2}} dz \tag{12}$$

denotes the optical depth of the layer at a height, z, and

$$\xi=5.5\times\frac{e^2}{\pi mc}\ln(220T/N_e^{1/3}) \tag{13}$$

has an almost constant value of 0.09 (in cgs units) in the solar chromosphere (ZHELEZNYAKOV 1970). The other symbols have their usual meaning.

For the coronal component of the emissions, we have

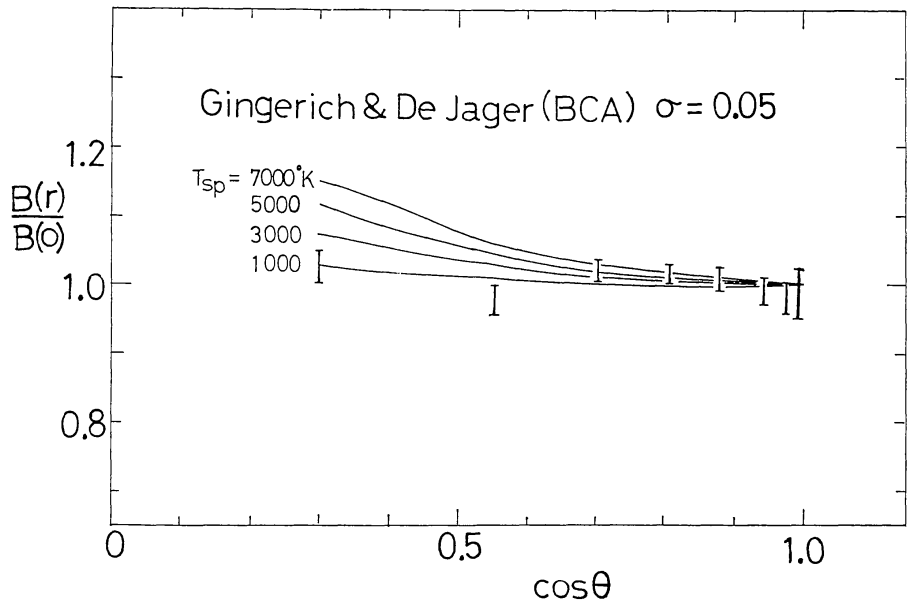

FIG. 4a. Center-to-limb variation of brightness at $\lambda=8.6$ mm. Vertical bars: Observations. The lengths of bars indicate probable errors. Solid lines: Calculated ones for various values of spicular electron temperature, T_{Sp}, and of σ, referring to the GINGERICH and DE JAGER (1968) model.

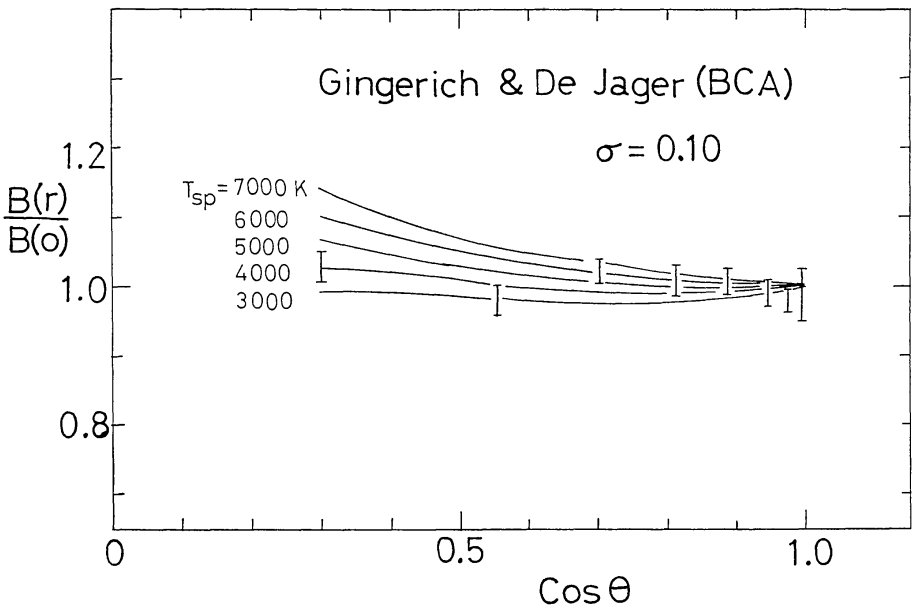

FIG. 4b. Same as Figure 4a but for $\sigma=0.10$.

$$T_{\mathrm{Cor}}=T\tau_{\mathrm{Cor}}\,, \tag{14}$$

where

$$\tau_{\mathrm{Cor}}=\frac{\xi}{\nu^2}\int\frac{N_e^2}{T^{3/2}}ds\,, \tag{15}$$

and

$$\xi=5.5\times\frac{e^2}{\pi mc}\ln\left(10^4T^{2/3}/N_e^{1/3}\right) \tag{16}$$

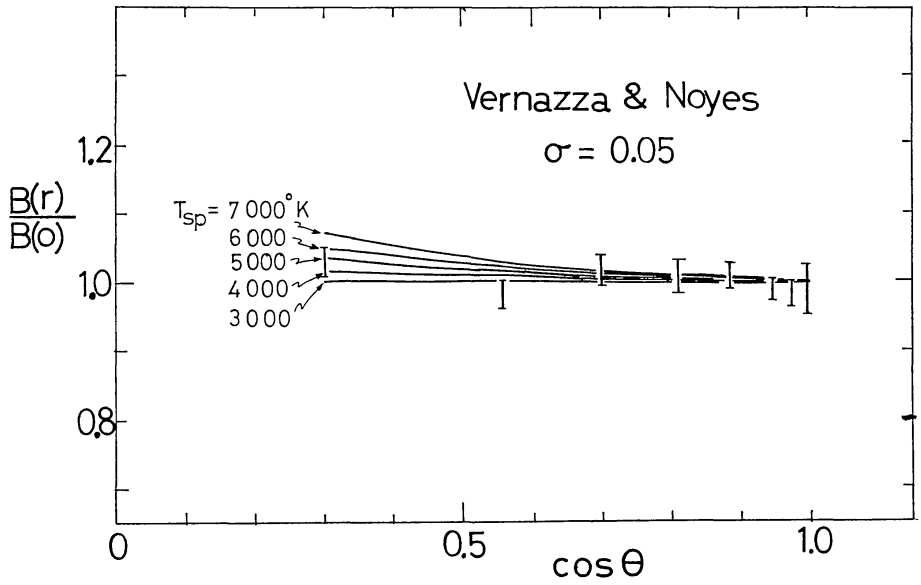

FIG. 4c. Same as Figure 4a but for the VERNAZZA and NOYES (1972) model with $\sigma=0.05$.

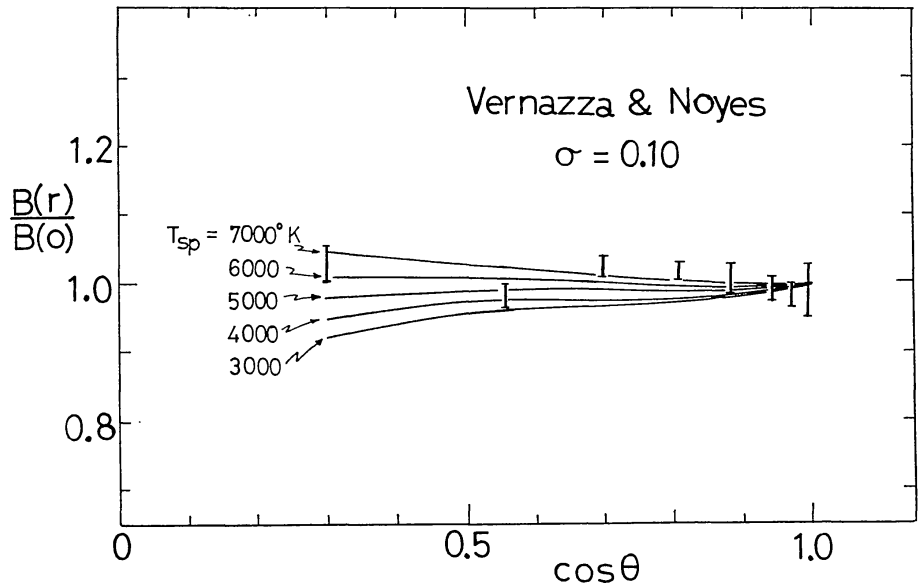

FIG. 4d. Same as Figure 4a but for the VERNAZZA and NOYES (1972) model with $\sigma=0.10$.

(ZHELEZNYAKOV 1970). Here the integration is carried out throughout the solar corona along the line of sight to the earth. ξ has a nearly constant value of about 0.24 in the coronal region. The electron temperature in the corona is assumed to be 10^6 K and the coronal electron density is assumed to be 1.4 times the Baumbach-Allen electron density (ALLEN 1947), which is about the same as that in the model of NEWKIRK (1967) and SAITO (1970).

TABLE 2. Best Fit Values of σ and T_{Sp}.

Model	σ	T_{Sp}(K)
GINGERICH and DE JAGER (1968, BCA)	0.10	4000
VERNAZZA and NOYES (1972)	0.05	4000
	0.10	6000

The brightness distribution at 8.6 mm is evaluated for various values of σ and T_{Sp}, by assuming the model chromosphere of GINGERICH and DE JAGER (1968; referred to as BCA) or by VERNAZZA and NOYES (1972) for the plane-parallel part of the chromosphere. These theoretical brightness distributions are illustrated in Figures 3 and 4, and are compared with observations. Table 2 summarizes the best fit values of σ and T_{Sp}.

As has been already mentioned, the component outside the limb is roughly in agreement with the coronal emissions. If we take a coronal electron temperature of 2×10^6 K, the coronal emissions decrease about 30 percent. It is, however, difficult to make a more precise comparison between the observed and calculated brightness of the coronal radio emissions because of a lack of the angular resolution.

Since spicules are assumed to be opaque at 8.6 mm, T_{Sp} is the same as the electron temperature within the spicules. As is seen in Figure 4a, the GINGERICH and DE JAGER (1968) model gives the electron temperature below 3000 K in the spicules for $\sigma=0.05$. Such a temperature is too low to be acceptable and then the spicular model with $\sigma=0.05$ will have to be excluded, in the case where the plane-parallel chromosphere in the interspicular region is close to the model of GINGERICH and DE JAGER (1968). Their model gives an electron temperature in the spicules as low as 4000 K even for $\sigma=0.10$ (Figure 4b). Referring to the model of VERNAZZA and NOYES (1972), the best fit with observations can be achieved if we adopt $T_{Sp}=4000$ K for $\sigma=0.05$ and $T_{Sp}=6000$ K for $\sigma=0.10$ (Figures 4c and 4d).

5. *Discussion*

The present investigation gives the electron temperature in the spicules below 6000 K for all cases described here. These values of the electron temperature agree with the low source function of the Lyman continuum radiations in the spicules as indicated by VERNAZZA and NOYES (1972) from considerations of the center-to-limb variations of the Lyman continuum.

The optical determination of the spicular temperature is still in controversy. BECKERS (1968) has derived 16000 K from intensity data of the spicular emission lines including helium lines. On the other hand, SUEMOTO (1963) has demonstrated that the spicular temperature is less than 9000 K from the line-width data. Recently, HIRAYAMA (1971) has suggested that helium lines will be excited by the coronal XUV radiations and has insisted that the spicular kinetic temperature must

be of 6000–8000 K in accordance with the widths of the Balmer lines and the turbulent velocities deduced from the metallic lines.

If we adopt the GINGERICH and DE JAGER (1968) model of the plane-parallel chromosphere in the interspicular region and reasonable values of σ, the spicular electron temperature becomes appreciably lower than all the optical determinations. Therefore, the GINGERICH and DE JAGER (1968) model must not be realistic in the interspicular region.

If we adopt the VERNAZZA and NOYES (1972) model, a spicular model with $\sigma=0.10$ gives a spicular electron temperature in good agreement with HIRAYAMA's (1971) determination, although we cannot rule out the case, $\sigma=0.05$, as being due to the lack of accuracy. Since the difference of the brightness distributions between various models are large only when close to the limb, high-resolution observations are needed to draw definite conclusions in these problems.

Remembering that spicules are assumed to be opaque at 8.6 mm, our arguments are correct only when the electron density is much higher than $10^{10}\,\mathrm{cm}^{-3}$ within spicules. The lower limit of the electron density within spicules does not contradict the electron density of $10^{11}\,\mathrm{cm}^{-3}$, indicated from the optical observations. If we adopt an electron density of $10^{11}\,\mathrm{cm}^{-3}$, it is inferred that spicules become transparent at wavelengths shorter than 3 mm and that the brightness distributions at these wavelengths have a limb brightening. The center-to-limb variations at 1.2 mm are still in controversy. NOYES, BECKERS, and LOW (1968) and NEWSTEAD (1969) have reported evidence of limb brightening. On the other hand, SHIMABUKURO (1971) has found no evidence of limb brightening and, furthermore, KUNDU (1971) has observed a limb darkening. If the limb darkening observed by KUNDU (1971) really exists, the electron density has to be higher than $10^{12}\,\mathrm{cm}^{-3}$ at least in the inner part of the spicules.

VERNAZZA and NOYES (1972) have suggested from considerations of the limb darkening observed by KUNDU (1971) at 1.2 mm that the electron temperature in spicules will be below 5200 K. A possible interpretation of the flat center-to-limb variation at 8.6 mm and the limb darkening at 1.2 mm is that the electron temperature is high, e.g. 6000 K, at the outer part of the spicules and low, e.g. below 5200 K in the inner part.

The authors wish to express their thanks to Mr. K. Akita for his assistance in the observations and data reduction. A part of the data analysis was carried out on a FACOM 230-60 at the Nagoya University.

References

Aeronomy and Space Data Center 1971, *Solar Geophys. Data* (U.S. Department of Commerce, Boulder, Colorado), No. 322, part 1, p. 39.

ALLEN, C.W. 1947, *Monthly Notices Roy. Astron. Soc.*, **107**, 406.

ALLEN, C.W. 1963, *Astrophysical Quantities* (Oxford University Press, New York), p. 174.

BECKERS, J.M. 1968, *Solar Phys.*, **3**, 367.

COATES, R.J. 1958a, *Proc. IRE*, **46**, 122.

COATES, R.J. 1958b, *Astrophys. J.*, **128**, 83.

COATES, R.J., GIBSON, J.E., and HAGEN, J.P. 1958, *Astrophys. J.*, **128**, 406.

DUNN, R.B. 1960, Ph. D. Thesis, Harvard University; *AFCRL Env. Res. Papers*, No. 109 (1965).

EL-RAEY, M. 1971, *Solar Phys.*, **16**, 404.

FLETT, A. M., FOSTER, P. R., STRACHAN, P., and THORNTON, D. C. 1971, *Solar Phys.*, **20**, 317.
GINGERICH, O., and DE JAGER, C. 1968, *Solar Phys.*, **3**, 5.
HAGEN, J. P. 1951, *Astrophys. J.*, **113**, 547.
HIRAYAMA, T. 1971, *Solar Phys.*, **19**, 384.
KUNDU, M. R. 1971, *Solar Phys.*, **21**, 130.
NEWKIRK, G. Jr. 1967, *Ann. Rev. Astron. Astrophys.*, **5**, 213.
NEWSTEAD, R. A. 1969, *Solar Phys.*, **6**, 56.
NOYES, R. W., BECKERS, J. M., and LOW, F. J. 1968, *Solar Phys.*, **3**, 36.
SAITO, K. 1970, *Ann. Tokyo Astron. Obs.*, **12**, 53.
SALOMONOVICH, A. E., PARIISKY, I. N., and KHANGIL'DIN, U. V. 1958, *Soviet Astron.*, **2**, 612.
SHIMABUKURO, F. I. 1970, *Solar Phys.*, **12**, 438.
SHIMABUKURO, F. I. 1971, *Solar Phys.*, **18**, 247.
SIMON, M. 1965, *Astrophys. J.*, **141**, 1513.
SIMON, M., BUHL, D., COGDELL, J. R., SHIMABUKURO, F. I., and ZAPATA, C. 1970, *Nature*, **226**, 1154.
SIMON, M., and ZIRIN, H. 1969, *Solar Phys.*, **9**, 317.
SUEMOTO, Z. 1963, *Publ. Astron. Soc. Japan*, **15**, 531.
TAKAHASHI, K. 1967, *Astrophys. J.*, **148**, 497.
TLAMICHA, A. 1969, *Solar Phys.*, **10**, 150.
TOLBERT, C. W., KRAUSE, L. C., and STRACHAN, A. W. 1964, *Astrophys. J.*, **140**, 306.
VERNAZZA, J. E., and NOYES, R. W. 1972, *Solar Phys.*, **22**, 358.
WHITHBROE, G. L. 1970, *Solar Phys.*, **11**, 208.
ZHELEZNYAKOV, V. V. 1970, in *Radio Emission of the Sun and Planets* (Pergamon Press, Oxford), p. 434.